

Cite this: *Phys. Chem. Chem. Phys.*,
2014, 16, 2417

Photophysics of a Schiff base: theoretical exploration of the excited-state deactivation mechanisms of *N*-salicyldenemethylfurylamine (SMFA)[†]

Ahmad J. Moghadam, Reza Omidyan* and Valiollah Mirkhani

Excited state reaction coordinates and the consequent energy profiles of a new Schiff base, *N*-salicydene-methylfurylamine (SMFA), have been investigated with the CC2 method, which is a simplified version of singles-and-doubles coupled cluster theory. The potential energy profiles of the ground and the lowest excited singlet state are calculated. In contrast to the ground state, the excited state potential energy profile shows a barrier-less dissociation pattern along the O–H stretching coordinate which verifies the proton transfer reaction at the S_1 ($\pi\pi^*$) state. The calculations indicate two S_1/S_0 conical intersections (CIs) which provide non-adiabatic gates for radiation-less decay to the ground state. At the CIs, two barrier-free reaction coordinates direct the excited system to the ground state of enol-type minimum. According to calculation results, a *trans*-keto type structure obtained from photoexcitation of the enol, can be responsible for the photochromic effect of SMFA. Furthermore, our results confirm the suggestion that aromatic Schiff bases are potential candidates for optically driven molecular switches.

Received 18th October 2013,
Accepted 11th November 2013

DOI: 10.1039/c3cp54416h

www.rsc.org/pccp

1. Introduction

The photophysics and chemistry of Schiff bases are important because they should be able to stand as good candidates for applications such as molecular switches and molecular memories.^{1–3} From the beginning of the 21th century, the search for molecular switches based on light-induced conformational changes has been a hot topic.^{3–10}

It is also well established that the optical properties of Schiff base molecules are related directly to their photochromic nature, which is a reversible reaction between enol and keto forms, giving rise to the reversible photocoloration of a single chemical species between two states.^{2,11} Recently, the photochromic effect of salicylaldehyde Schiff bases have been the subject of several papers,^{3,12–17} where it was demonstrated that the excited state intramolecular proton transfer (ESIPT) process after photo excitation is the most crucial step in excited state reaction dynamics of these molecules.^{18–20} Beyond this process, producing a keto structure as a new tautomeric form is responsible for photochromic effect with bathochromically shifted spectra.^{12,13}

So far, the ESIPT has attracted massive research interest, both in theory and experiment.^{21–25} Although, a repulsive $\pi\sigma^*$ state

plays the prominent role on hydrogen or proton detachment processes in organic compounds,^{7,26} the $\pi\pi^*$ excited electronic state leads the excited systems involving an intramolecular hydrogen bond to ESIPT.^{27–29} Also, the excited $\pi\pi^*$ state, plays the most crucial step on the photophysics of Schiff bases by proton transfer (PT) from hydroxyl to the amino group.^{15,16,18,19,30,31}

In contrast to the importance of photoproducts and photophysics of Schiff bases, very little is known about the excited states of such important compounds.^{13,15–17} Recently, Spörkel and coworkers³² reported a theoretical study on a salicylidene-aniline Schiff base molecule, where, they demonstrated that the S_1 *cis*-keto conformer is responsible for fluorescence, especially in rigid surroundings and a proton transfer from the S_0 state (enol) to S_1 state (*cis*-keto) occurs when the molecule is planar, and flexibility of the molecule is essential for achieving photochromic activity of Schiff bases. Also, the latest studies on the photophysical behavior of small Schiff bases established that beyond the ESIPT process, conical intersections between the S_1/S_0 energy profiles bring about several depopulation routes including back proton transfer and photo-isomerization.^{12,13} These deactivation pathways lead the excited system to its original state, resulting in a large portion of molecules being trapped in the ground state as metastable photochromic species.^{12,13} Furthermore, according to the CC2 and TD-DFT calculation results of Jankowska *et al.*,¹³ it was demonstrated that four photophysically relevant isomeric forms from irradiation of salicylidene-methylamine (SMA), are responsible for the photochromic effects of

Department of Chemistry, University of Isfahan, 81746-73441, Isfahan, Iran.

E-mail: r.omidyan@sci.ui.ac.ir, reza.omidyan@u-psud.fr; Fax: +98 311 6689732

[†] Electronic supplementary information (ESI) available. See DOI: 10.1039/c3cp54416h

this compound. These isomers are populated from the conical intersections between potential energy surfaces, and they have main contributions to the UV-vis absorption spectrum of SMA, in agreement with experimental observations.¹⁹ Also, it was shown that CC2 calculations are reliable in the prediction of UV-vis absorption spectra and interpretation of photophysical behavior of Schiff base molecules.¹³

In the present work, we will report the PE functions obtained by the CC2 method for ESIPT and detail mechanisms on the formation of the photochromic tautomer of SMFA. In particular, we focus on conical intersections (CIs)³³ which are relevant for the photoinduced reactions of SMFA. Photo-isomerization and internal conversion through CIs which are reached by the twisting of CN and CC double bonds are widely accepted paradigms for ultrafast radiation-less decay in Schiff Bases.^{12,13} The UV-vis absorption spectra of global minima and photo induced tautomers of SMFA are explored in the present work. CC2 is the method of choice because it gives reasonable results for medium size organic molecules, for a moderate computational time.^{34–44}

2. Computational details

The *ab initio* calculations were performed with the TURBOMOLE program package.^{45,46} The resolution-of-the-identity Møller–Plesset perturbation theory⁴⁷ to second-order (RI-MP2)^{48,49} calculations were performed to obtain the equilibrium geometry of all molecules at the ground electronic state. The vertical electronic absorption spectra were calculated with the CC2^{50,51} method using

correlation consistent double- ζ (cc-pVDZ) and the augmented cc-pVDZ⁵² basis sets on the MP2/cc-pVDZ optimal structures.

Since CC2 is the method of choice for investigation of excited-state minimum-energy reaction paths, thanks to an effective implementation of analytical gradients, the required calculations for determination of potential energy curves were performed with the correlation-consistent polarized valence double- ζ (cc-pVDZ) basis set. In order to optimize the excited state geometries, the MP2 optimized geometries have been chosen as the starting point of the calculations.

The abbreviations of SMFA and **5a** are being used, respectively, as alternatives of 2-(hydroxybenzyl-2-furylmethyl) imine and its most stable configuration enol form. Finally, charge distribution calculations were performed based on the Natural Population Analysis algorithm (NPA)⁵³ implemented on the TURBOMOLE program package.

3. Results and discussion

3.1. Ground state structures

The first step of this work is looking for the most stable structure of SMFA. By a quick glance at the geometry of any rotamer of the SMFA (see Fig. 1), one can predict several possibilities for taking orientations by the methyl-furyl part of the molecule with respect to a planar structure of salicylaldehyde. This planar arrangement is more favoured for salicylaldehyde due to intramolecular hydrogen bonding (OH...NC).^{54–59} However, according to the flexibility of the furyl-methyl part of SMFA, one may consider several rotamers

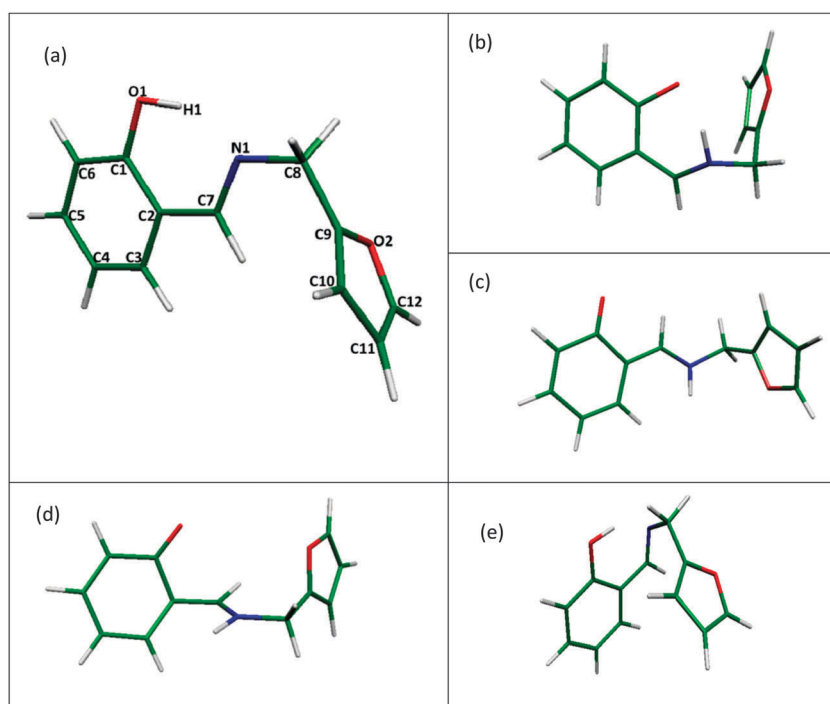
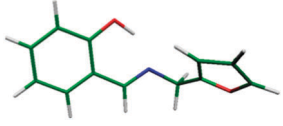
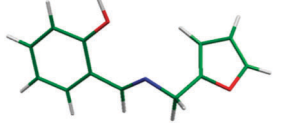
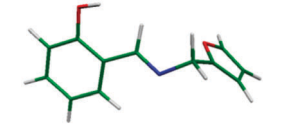
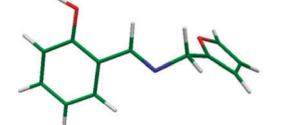
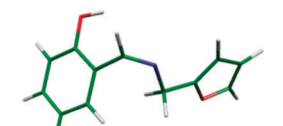
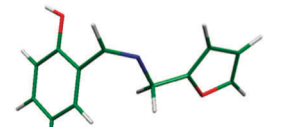
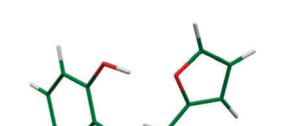
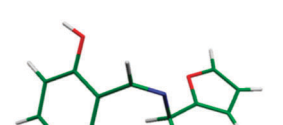
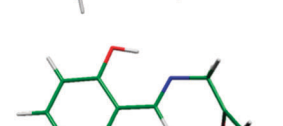
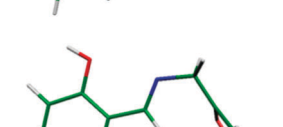
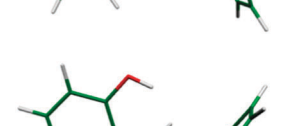
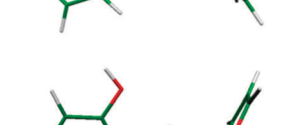
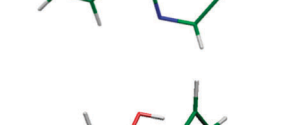
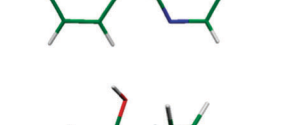
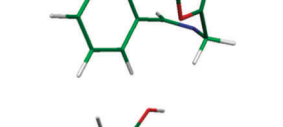
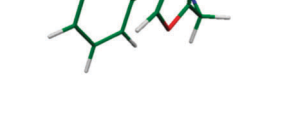


Fig. 1 The optimized geometries and the numbering pattern: (a) the most stable configuration of the enol form of **5a** (calculated at the MP2/cc-pVDZ level of theory). (b) The S_1 optimized structure of the *cis*-keto form of **5a** (determined at the CC2/cc-pVDZ level of theory). (c) The optimized geometry structure of **5d**, *trans*-keto form of SMFA obtained at the MP2/cc-pVDZ level of theory. (d) and (e) Qualitative geometry of the S_1 – S_0 conical intersections of CI-1 and CI-2 respectively.

for this molecule. Although our goal is not to evaluate the geometry properties of all isomers or rotamers associated with this molecule, several of the most probable configurations have been examined in our work and the optimized geometry of these rotamers have been determined. The optimized structures, along with their energetic ground state levels with respect to the most stable conformer of **5a** are presented in Table 1. Of course,

most of these rotamers could be obtained either by rotation of N1–C8 around the C2–C7 or by rotation of C9–C8 around the N1–C7 bond. Although, there is only one rotamer (nominally **1a**) which is only 0.03 eV (2.9 kJ mol^{−1}) less stable than **5a**, the energetic ground state level of other rotamers is at least 0.43 eV (41.50 kJ mol^{−1}) higher than that of the most stable rotamer of **5a**, thus we ignore performing more calculations on these molecules.

Table 1 Optimized geometry and relative ground state energy of several rotamers of SMFA. The values in parenthesis (in eV), represent the difference between the internal energy associated with each rotamer and the most stable configuration of SMFA (**5a**). The calculations have been performed at the MP2/cc-pVDZ level of theory

Rotamer	Optimized geometry	Rotamer	Optimized geometry
1a (0.03)		1b (0.6)	
2a (0.50)		2b (0.43)	
3a (0.69)		3b (0.68)	
4a (0.55)		4b (0.71)	
5a (0.0)		5b (0.60)	
6a (0.48)		6b (0.43)	
7a (0.61)		7b (0.66)	
8a (0.60)		8b (0.67)	

(Details on the xyz coordinates of rotamers and tautomers of SMFA are presented in Tables SM1 and SM2, ESI†.)

In agreement with our previous work,¹² using the MP2 calculations, no minimum has been found for the *cis*-keto tautomer of SMFA, due to back proton transfer from N1 to O1 and producing the global minimum enol form. While the MP2 calculation shows that the *trans*-keto is stable at the ground state, its energetic level (0.83 eV) is significantly higher than the original minimum of the most stable enol configuration (see Fig. 1c). Similar to the enol form of SMFA, various rotamers for the *trans*-keto structure could be considered. Nonetheless, analyzing the rotamers and tautomers is away from the main subject of this work.

3.2. Excited state geometry and electronic properties

The vertical excitation energy at the CC2 level using cc-pVDZ and aug-cc-pVDZ basis sets on the S_0 geometry of two enol form rotamers (**5a** and **1a**), for which the nearest ground state energies have been determined, and also one *trans*-keto

tautomer of SMFA have been calculated. The results are presented in Table 2. As shown the vertical transition energies associated with **5a** and **1a** rotamers are quite close to each other and the oscillator strengths show the same trend. Considering the vertical excitation energies of these rotamers, the SMFA identifies two strong electronic transitions: the S_1 - S_0 transition lies between 4.07–4.11 (305–302 nm), with oscillator strength of 0.118, and can be described as the $\pi\pi^*$ (H–L) excitation, (H and L indicate the HOMO and LUMO, respectively). The S_3 - S_0 lies at 5.13–5.17 eV (242.1–232.6 nm) with the oscillator strength of 0.181. Specially, one electron excitations that contribute to this transition are (H – 2)–L, which could be assigned mainly to the $\pi\pi^*$ too. However, the weakest transition is S_2 - S_0 , which has $n\pi^*$ character, which corresponds to the electronic transition of (H – 4)–L with the oscillator strength of 0.001. The S_4 - S_0 ($\pi\pi^*$) electronic transition consists of H – 1–L and is also too weak (see Table 3).

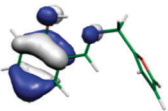
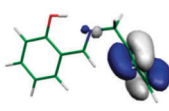
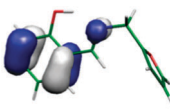
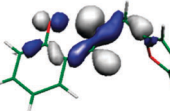
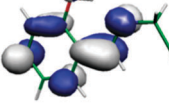
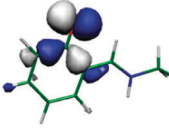
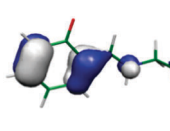
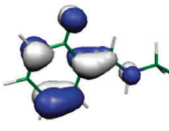
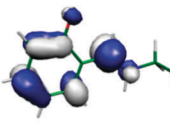
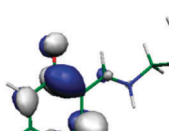
Concerning the photochromic properties of SMFA, other tautomers should be involved in the UV-visible absorption spectrum. Thus, we calculated the vertical excitation energies at the same level of theory on the MP2 ground state optimized geometry merely for the *trans*-keto tautomer of **5a** (nominated to **5d**). The calculations at the CC2/aug-cc-pVDZ level, indicate two strong electronic transitions; the S_2 - S_0 transition at the 3.04 eV (408.55 nm), can be described as the $\pi\pi^*$ (H–L) excitation (see Table 3). The oscillator strength of this transition is 0.300. The S_4 - S_0 transition also lies at 4.61 eV (268.8 nm) with the oscillator strength of 0.155, and can be described as $\pi\pi^*$ since there is one electron excitation of H–(L + 4). At the CC2 level, the weakest transition is S_1 - S_0 , which has $n\pi^*$ nature corresponding to the electronic transition of (H – 3)–L with the oscillator strength of 0.003.

The CC2 geometry optimization of **5a** at the first singlet excited state (S_1) shows an excited state proton transfer from the hydroxyl group to the imine of SMFA. The calculated charge distributions at the ground and S_1 excited state of **5a** show slight charge transfer character along with the S_1 - S_0 excitation. The total charge transferred from the phenolic part of the SMFA toward the rest is $-0.04q$ (see Table SM3 in the ESI†).

Table 2 Vertical energy gap (eV) and oscillator strength (f) of the **5a** and **1a** enol and *trans*-keto forms, calculated at the crucial points of the ground state potential energy surface with the CC2 method, using cc-pVDZ and aug-cc-pVDZ basis sets

State	cc-pVDZ	aug-cc-pVDZ	f
5a (enol, 0.00 eV)			
S_1 ($\pi\pi^*$)	4.19	4.11	0.1180
S_2 ($n\pi^*$)	5.09	4.94	0.0010
S_3 ($\pi\pi^*$)	5.39	5.17	0.1810
S_4 ($\pi\pi^*$)	6.07	5.43	0.0040
5d (<i>trans</i> -keto, 0.83 eV)			
S_1 ($n\pi^*$)	3.03	2.90	0.0034
S_2 ($\pi\pi^*$)	3.28	3.04	0.3004
S_3 ($n\pi^*$)	4.88	4.46	0.0050
S_4 ($\pi\pi^*$)	5.60	4.61	0.1552
1a (enol, 0.03 eV)			
S_1 ($\pi\pi^*$)	4.15	4.07	0.1060
S_2 ($n\pi^*$)	5.13	5.00	0.0040
S_3 ($\pi\pi^*$)	5.36	5.13	0.1810
S_4 ($\pi\pi^*$)	5.51	5.24	0.0080

Table 3 The frontier molecular orbitals of the most stable conformation of enol and *trans*-keto forms of the SMFA

5a (enol form of SMFA)				
HOMO	HOMO – 1	HOMO – 2	HOMO – 4	LUMO
				
5d (<i>trans</i> -keto form)				
HOMO – 3	HOMO – 2	HOMO	LUMO	LUMO + 4
				

These calculations may verify that the ESIPT is consequently electron driven.¹²

3.3. Potential energy profiles and internal conversions

One may wonder whether the **5a** rotamer is the most stable configuration for SMFA or is there still another structure with the lower ground state energy? To look for the answer to this question, we examined the minimum potential energy profiles relevant to the flexible methyl-furyl part of SMFA, along with the reaction coordinates of α ; (the dihedral angle of C7–N1–C8–C9) and β ; (the dihedral angle of N1–C8–C9–O2). The results are presented in Fig. 2a and b respectively. Fig. 2a shows two minima at the $\alpha = 0^\circ$ and 120° in the minimum energy profile of SMFA along the dihedral angle C7–N1–C8–C9. These minimum-points can be assigned to the rotamers of **5a** and **1a** respectively (see Table 1). Fig. 2(b), shows the minimum energy profile of **5a** along the reaction coordinates of β (the dihedral angle of N1–C8–C9–O2). As shown, the MEP shows only one minimum at $\beta = 85^\circ$, corresponding to the optimized structure of **5a** as well. Inspection of Fig. 2, verifies that the optimized geometry of **5a** is located in the minimum of PES along both α and β reaction coordinates.

According to the ground state energy levels associated with the MP2 optimized geometries for several structures involved in the calculations (Table 1), and also considering the MPE profiles of Fig. 2a and b, it has been concluded that the most stable structure for SMFA is **5a** and all of the other rotamers lie

in the higher ground state level of energy. Thus the rotamer of **5a** has been selected for more photophysical and chemical investigations in this work. This molecular system displays a strong absorption at 4.11 eV in the first excited state with $\pi\pi^*$ character. Also, its associated geometric parameters are presented in Table SM4 (ESI[†]).

According to the CC2 geometry optimization of **5a** at the first singlet excited state (S_1), the enol form of this molecule converts to a keto form that is less stable than the global minimum by about 3 eV. In addition to proton detachment and attachment from hydroxyl to amino group, the S_1 optimization lead to significant alternations in geometry parameters; for instance the C2–C7–N1–C8 dihedral angle decreases from 179.68° to -129.167° and the C1–C2–C7–N1 dihedral angle increases from -1.00° to 22.99° (see Table SM4, ESI[†]).

The minimum potential energy (MPE) profiles of **5a** in the S_0 state and in the lowest excited $1\pi\pi^*$ state, determined along the PT (OH distance) and along the torsion of the ethyl-furyl group (dihedral angle of $\varphi(\text{C2–C7–N1–C8})$) and of the methylamine group (dihedral angle of $\omega(\text{C1–C2–C7–N1})$) are shown in Fig. 3.

The middle panel of Fig. 3, illustrates that the enol form of **5a** is a typical excited-state intra molecular proton transfer (ESIPT) system. The minimum energy profiles (full lines) were obtained by optimization of molecular geometry for fixed values of the reaction coordinate for ground and excited states, performed respectively at the MP2/cc-pVDZ or CC2/cc-pVDZ level of theory. In addition, the vertical PE profiles of the ground state calculated at the optimized geometry of a given excited state were determined (dashed lines). Hence $S_0(\pi\pi^*)$ denotes the energy of the S_0 state calculated along the reaction path optimized in the $\pi\pi^*$ state, and so forth. The results showed that after optical excitation of **5a** to the first excited singlet state ($\pi\pi^*$), a spontaneous (barrier-free) PT reaction occurs.

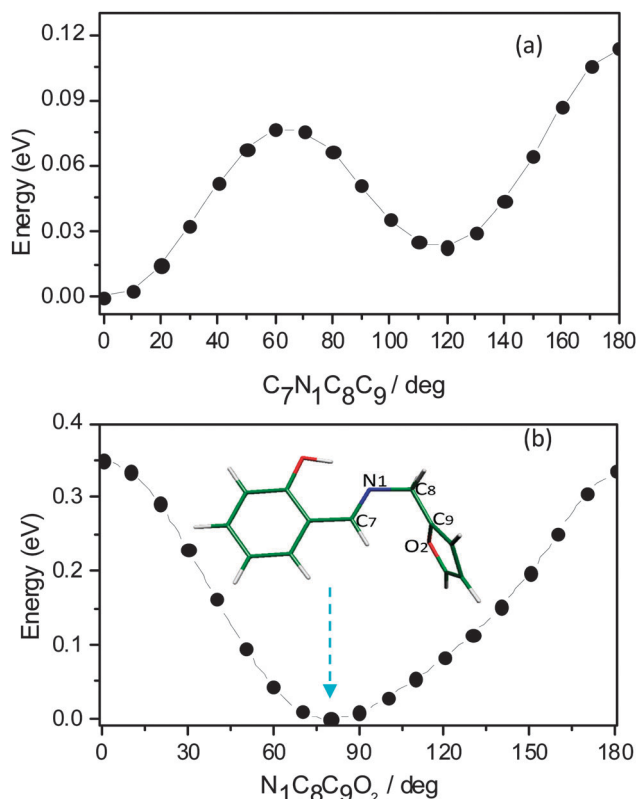


Fig. 2 Energy profile of the S_0 state of the **5a** form of SMFA as the function of (a) the C7–N1–C8–C9 dihedral angle and (b) the N1–C8–C9–C10 dihedral angle, computed at the MP2/cc-pVDZ level of theory.

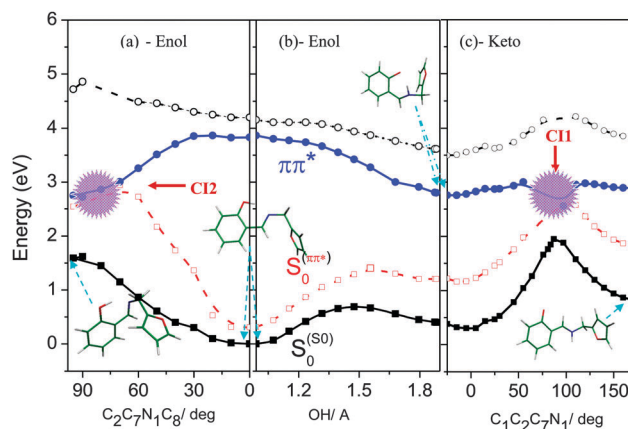


Fig. 3 Energy profiles of SMFA in the S_0 state (squares) and $S_1(\pi\pi^*)$ state (circles) as a function of the torsional reaction path (a and c) and the hydrogen transfer reaction path (b), determined at the CC2/cc-pVDZ level (MP2/cc-pVDZ for the ground state). Full lines: energy profiles of reaction paths determined in the same electronic state ($S_0^{(S_0)}$, $S_1^{(\pi\pi^*)}$). Dashed lines: energy profiles of reaction paths determined in the complementary electronic state ($S_0^{(\pi\pi^*)}$, $S_1^{(S_0)}$). Shaded stars denote area where the CC2 iteration cycle ceases to converge due to degeneracy of the S_1 and the S_0 states.

Although the C2–C7 bond is a single bond in the enol form (5a), after the proton transfer, it changes into a double bond of *cis*-enol form. Considering the MPE curve of the ground state in Fig. 3(b), the enol–keto transformation is not favored any more in the ground state, while in the S_1 ($\pi\pi^*$) state, the PES does not show a barrier, and this transformation will be favored by decreasing the internal energy of the system along the enol–keto transformation. It verifies that spontaneous hydrogen transfer takes place on the S_1 ($\pi\pi^*$) state, resulting in the formation of the keto tautomer on the excited state potential energy surface. The keto-type S_1 structure is estimated to lie 2.80 eV (CC2 result) above the global minimum of the ground state (see Fig. 3(b)).

Previous calculations for PT systems have shown that the torsion of the proton-accepting group relative to the proton donating group plays an essential role for the effective quenching of the electronic excitation in these systems.^{12,13} Fig. 3(c) shows the energy profiles for the MEP associated with the torsion of the amino group. Although we didn't find a ground state minimum for the case of *cis*-keto structure of SMFA, this photoproduct of SMFA is presumably a longer-lived species than the corresponding *cis*-keto structure previously studied in the cases such as SBEA¹² and SMA,¹³ because there is a small barrier of 0.25 eV for rearrangement of *cis*-keto to *trans*-keto tautomer (Fig. 3c). In the S_1 state, the MEP for amino torsion could be determined with the exception of geometries, which are very close to the S_1 – S_0 conical intersection ($50^\circ < \omega < 100^\circ$), where the CC2 iteration cycle fails to converge. One may notice upon inspection of Fig. 3(c) that while the twist brings a large increase in the ground-state energy, the excited-state energy seems to remain almost constant. As a result, when ω lies in the range 55° – 97° and 97° – 110° , the ground- and excited-state energies computed at the optimized excited-state geometry sharply approach each other, and in the range 55° – 110° the CC2 iteration cycle in almost all calculations ceases to converge.

The CC2 method, being a single-reference method, is expected to fail in the vicinity of the intersection of excited states with the electronic ground state. The corresponding regions of the PE profiles are given by shaded stars in Fig. 3, indicating that these data are less reliable. The accurate calculation of the PE surfaces in the immediate vicinity of S_1 – S_0 conical intersections requires multi-reference methods, in particular state-averaged CASSCF and MR perturbation or configuration-interaction methods, however, the CC2 prediction only for the CI regions could be reliable.^{13,28,60–62}

Similar PE profiles are obtained when the reaction path is chosen as the dihedral angle of $\theta(\text{C2}–\text{C7}–\text{N1}–\text{C8})$, which is shown in the left panel of Fig. 3. Unlike in the case discussed for the keto structure of 5a, there is neither a stable point in the S_1 nor in the S_0 state after the conical intersection between S_1/S_0 along the MEP for the enol form of 5a in this reaction coordinate.

The MEP of the ground state computed along the first twisting (dihedral angle of $\theta(\text{C1}–\text{C2}–\text{C7}–\text{N1})$) coordinates shows remarkable barrier (~ 2 eV) near the perpendicular orientation of the relevant double bonds which separate the MP2 optimized enol form of 5a and optimized *trans*-keto of this compound.

The above finding indicates the presence of a S_1/S_0 conical intersection (CI) in the vicinity of the perpendicular twisting of the C7–N1 and C2–C7 double bonds of the respective enol and keto forms of 5a. Because the CC2 method is a single reference method, it is not convenient to precisely predict the geometry of CI, but it can be approximately estimated as shown in Fig. 1.

Moreover, the latter pathway would encompass the rotation of two parts of the molecule which are both heavier than the proton particle and thus, the evolution of the system along the twisting coordinate is expected to be much slower than that along the PT coordinate.

A barrier-less PE profile of the S_1 ($\pi\pi^*$) state in the direction of the PT reaction and the small mass of the proton leads to the conclusion that the photophysics of SMFA is dominated by the ESIPT reaction which eventually may result in the formation of the photochromic *trans*-keto form.

However, the reaction pathway leading to the CI-2, is also barrier-less and it plays an essential role in the photochemical behavior of SMFA after excitation. Since a large steric hindrance exists when $\varphi > 95^\circ$, we didn't find a local minimum for the ground state along with this reaction coordinate. Therefore, this reaction coordinate should only act as a radiation-less deactivation pathway of the S_1 ($\pi\pi^*$) state to the ground state *via* the CI-2.

Similar PE profiles are obtained when optimizing the reaction paths connecting 5a and 6a along the dihedral angle of $\zeta(\text{C1}–\text{C2}–\text{C7}–\text{N1})$ which is shown in Fig. 4. The $S_0^{(SO)}$ curve exhibits the barrier for torsion of imine group in the S_0 state of SMFA ($E \approx 0.8$ eV). The energy profile of the S_1 ($\pi\pi^*$) state calculated along the S_1 ($\pi\pi^*$) reaction path in Fig. 4 indicates an increase of this barrier (up to 1.5 eV) in the S_1 state. Once more, the CC2 method doesn't work appropriately in the region of ζ between 55° – 95° . This part of the PE function is represented by the dashed line in Fig. 4 (red and blue colours). The MEP in the S_1 state could be determined for other dihedral angles ($55^\circ > \varphi > 95^\circ$) too.

In addition, one important point to clarify that, is the relation between rotamers–tautomers of SMFA and its

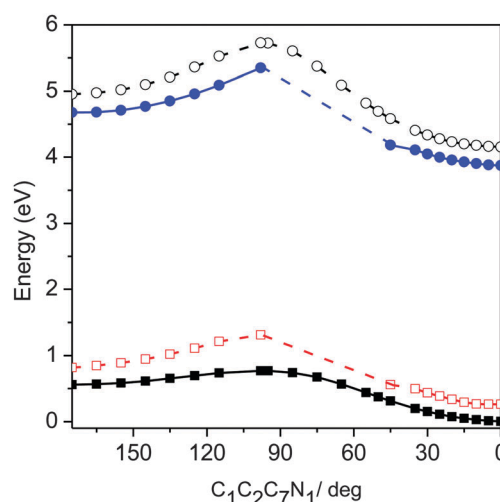


Fig. 4 As Fig. 3. PE profiles as a function of the torsional reaction path of C1–C2–C7–N1 in the enol form of 5a.

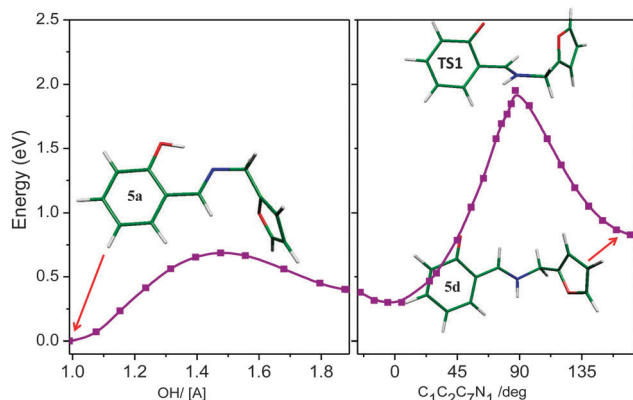


Fig. 5 Energy profiles of SMFA in the S_0 state determined at the MP2/cc-pVDZ level along the minimum-energy path for: proton transfer (OH stretching) and the C1C2C7N1 single-bond twist in the enol form of **5a**.

photochromic properties. In order to illustrate the energetic relation between the isomers of **5a** and **5d**, and also TS_1 , which are the most important photochromic and photophysical species of SMFA, a one-dimensional minimum-energy cut through the PES that connects TS_1 with the **5d**-form is shown in Fig. 5. Because of the large barrier between the *cis*-enol and *trans*-keto (**5a** and **5d** respectively) for rotation around the double bonds, an interconversion between different rotamers can only be induced photophysically. Fig. 3 indicates two photophysically relevant CIs (CI-1 and CI-2) which provide non-adiabatic gates for a radiation-less decay to the ground state. Internal conversions through these CIs, from both sides of Fig. 3, populate the ground state of SMFA at the conformations near to CI1 and CI2. The twisted structure at the CI1, (TS_1 structure in Fig. 5), can be assigned to the transient structures for the formation of the **5d** isomer from the native **5a**-form. In contrast to CI-1, which populates a photochromic species nominally in the *trans*-keto form (**5d**), from CI2, no minimum except that of **5a** could be accessed. The high steric hindrance between the ethyl-furyl moiety and the phenolic part of SMFA prevents increasing the dihedral angle of $\zeta(C2-C7-N1-C8)$ to more than 90° and the MEP of the ground state at this point only leads the molecule to the minimum point (**5a**). Thus the preferred photophysical behavior in CI2 is a relaxation to the ground state of **5a**.

At CI-1, where an internal convergence (IC) to the ground state takes place, the system has a much higher energy (≈ 2.5 eV), that can pass the small barrier located in the back-proton transfer region. In addition, the internal energy of TS_1 is high enough to populate the photochromic **5d**-form as well.

4. Conclusion

The computational results of the present work suggest the following features of the photophysics of SMFA. This molecule is transparent to visible radiation but strongly absorbent for UV radiation. The primary UV-induced reaction is proton transfer from the hydroxyl group to the imine group. This reaction is predicted to be essentially barrier-less and thus extremely fast.

The photochromic species SMFA formed in this process absorbs strongly in the visible range of the spectrum. It represents a typical example of a so-called ESIPT system. The characteristic features of such systems are strong and broad absorption in the UV/vis range, and very fast radiation-less return to the ground state. Such systems effectively convert the photon energy into vibrational energy (heat), as is well known for commercially used photostabilizers and photoscreens. The calculations indicate that the *trans*-keto form (**5d**) produced by UV excitation of **5a** is a strong UV/vis absorber and should be highly photostable. Upon strong UV irradiation, a significant concentration of the *trans*-keto form of SMFA (**5d**) can be produced. This form absorbs strongly in the visible range of the spectrum. The ground state of the *trans*-keto form (**5d**) is metastable ($\Delta E = 0.84$ eV). The thermal back reaction from **5d** to the more stable **5a** has to overcome a barrier of about 1.1 eV and is therefore expected to be rather slow. Thus, UV irradiation of SMFA may result in a mixture of **5a** and its photoproduct **5d**.

Acknowledgements

The research council of Isfahan University is gratefully acknowledged. We also kindly appreciate the use of computing facility cluster GMPCS of the LUMAT federation (FR LUMAT2764) in France for performing some parts of our calculations.

References

- 1 J. M. Tour, *J. Am. Chem. Soc.*, 1996, **118**, 2309–2310.
- 2 H. Dürr and H. Bouas-Laurent, *Photochromism: Molecules and Systems: Molecules and Systems*, Access Online via Elsevier, 2003.
- 3 S. Pu, Z. Tong, G. Liu and R. Wang, *J. Mater. Chem. C*, 2013, **1**, 4726–4739.
- 4 C.-J. Xia, D.-S. Liu, H.-C. Liu and Y.-T. Zhang, *Mol. Phys.*, 2010, **109**, 209–215.
- 5 J. M. Ortiz-Sanchez, R. Gelabert, M. Moreno and J. M. Lluch, *J. Chem. Phys.*, 2008, **129**, 214308–214311.
- 6 A. Migani, L. s. Blancafort, M. A. Robb and A. D. DeBellis, *J. Am. Chem. Soc.*, 2008, **130**, 6932–6933.
- 7 A. L. Sobolewski and W. Domcke, *J. Phys. Chem. A*, 2007, **111**, 11725–11735.
- 8 A. L. Sobolewski, W. Domcke and C. Hättig, *J. Phys. Chem. A*, 2006, **110**, 6301–6306.
- 9 J. M. Ortiz-Sánchez, R. Gelabert, M. Moreno and J. M. Lluch, *J. Phys. Chem. A*, 2006, **110**, 4649–4656.
- 10 I. Gómez, M. Reguero, M. Boggio-Pasqua and M. A. Robb, *J. Am. Chem. Soc.*, 2005, **127**, 7119–7129.
- 11 E. Hadjoudis, S. D. Chatziefthimiou and I. M. Mavridis, *Curr. Org. Chem.*, 2009, **13**, 269–286.
- 12 A. J. Moghadam, R. Omidyan, V. Mirkhani and G. Azimi, *J. Phys. Chem. A*, 2013, **117**, 718–725.
- 13 J. Jankowska, M. F. Rode, J. Sadlej and A. L. Sobolewski, *ChemPhysChem*, 2012, **13**, 4287–4294.

- 14 M. Z. Zgierski, T. Fujiwara and E. C. Lim, *Chem. Phys. Lett.*, 2008, **463**, 289–299.
- 15 M. Z. Zgierski, *J. Chem. Phys.*, 2001, **115**, 8351–8358.
- 16 M. Z. Zgierski and A. Grabowska, *J. Chem. Phys.*, 2000, **112**, 6329–6337.
- 17 M. Z. Zgierski and A. Grabowska, *J. Chem. Phys.*, 2000, **113**, 7845–7852.
- 18 M. Ziolek, J. Kubicki, A. Maciejewski, R. Naskrecki and A. Grabowska, *Phys. Chem. Chem. Phys.*, 2004, **6**, 4682–4689.
- 19 J. Grzegorzec, A. Filarowski and Z. Mielke, *Phys. Chem. Chem. Phys.*, 2011, **13**, 16596–16605.
- 20 M. Ziolek, G. Burdzinski, K. Filipczak, J. Karolczak and A. Maciejewski, *Phys. Chem. Chem. Phys.*, 2008, **10**, 1304–1318.
- 21 A. P. Demchenko, K.-C. Tang and P.-T. Chou, *Chem. Soc. Rev.*, 2013, **42**, 1379–1408.
- 22 J. Zhao, S. Ji, Y. Chen, H. Guo and P. Yang, *Phys. Chem. Chem. Phys.*, 2012, **14**, 8803–8817.
- 23 I. Presiado, Y. Erez, R. Gepshtein and D. Huppert, *J. Phys. Chem. C*, 2010, **114**, 3634–3640.
- 24 H. Langer, N. L. Doltsinis and D. Marx, *ChemPhysChem*, 2005, **6**, 1734–1737.
- 25 S. Scheiner, *J. Phys. Chem. A*, 2000, **104**, 5898–5909.
- 26 A. L. Sobolewski and W. Domcke, *J. Phys. Chem. A*, 2001, **105**, 9275–9283.
- 27 S. Yamazaki, A. L. Sobolewski and W. Domcke, *Phys. Chem. Chem. Phys.*, 2011, **13**, 1618–1628.
- 28 A. L. Sobolewski and W. Domcke, *Phys. Chem. Chem. Phys.*, 2006, **8**, 3410–3417.
- 29 A. L. Sobolewski and W. Domcke, *Phys. Chem. Chem. Phys.*, 1999, **1**, 3065–3072.
- 30 C. Randino, M. Ziolek, R. Gelabert, J. A. Organero, M. Gil, M. Moreno, J. M. Lluch and A. Douhal, *Phys. Chem. Chem. Phys.*, 2011, **13**, 14960–14972.
- 31 E. Hadjoudis and I. M. Mavridis, *Chem. Soc. Rev.*, 2004, **33**, 579–588.
- 32 L. Spörkel, G. Cui and W. Thiel, *J. Phys. Chem. A*, 2013, **117**, 4574–4583.
- 33 W. Domcke, D. R. Yarkony and H. Kèoppel, *Conical intersections: electronic structure, dynamics and spectroscopy*, World Scientific, 2004.
- 34 M. Schreiber, M. R. Silva-Junior, S. P. Sauer and W. Thiel, *J. Chem. Phys.*, 2008, **128**, 134110.
- 35 I. Alata, J. Bert, M. Broquier, C. Dedonder, G. Feraud, G. Gregoire, S. Soorkia, E. Marceca and C. Juvet, *J. Phys. Chem. A*, 2013, **117**, 4420–4427.
- 36 I. Alata, M. Broquier, C. Dedonder, C. Juvet and E. Marceca, *Chem. Phys.*, 2012, **393**, 25–31.
- 37 I. Alata, C. Dedonder, M. Broquier, E. Marceca and C. Juvet, *J. Am. Chem. Soc.*, 2010, **132**, 17483–17489.
- 38 I. Alata, R. Omidyan, M. Broquier, C. Dedonder, O. Dopfer and C. Juvet, *Phys. Chem. Chem. Phys.*, 2010, **12**, 14456–14458.
- 39 I. Alata, R. Omidyan, M. Broquier, C. Dedonder and C. Juvet, *Chem. Phys.*, 2012, **399**, 224–231.
- 40 I. Alata, R. Omidyan, C. Dedonder-Lardeux, M. Broquier and C. Juvet, *Phys. Chem. Chem. Phys.*, 2009, **11**, 11479–11486.
- 41 A. L. Sobolewski and L. Adamowicz, *J. Phys. Chem.*, 1996, **100**, 3933–3941.
- 42 G. Grégoire, C. Juvet, C. Dedonder and A. L. Sobolewski, *J. Am. Chem. Soc.*, 2007, **129**, 6223–6231.
- 43 A. L. Sobolewski, D. Shemesh and W. Domcke, *J. Phys. Chem. A*, 2008, **113**, 542–550.
- 44 N. Solcà and O. Dopfer, *J. Phys. Chem. A*, 2003, **107**, 4046–4055.
- 45 *Turbomole, a development of the University of Karlsruhe and Forschungszentrum Karlsruhe GmbH, 1989–2007, Turbomole, GmbH, since 2007; available from* <http://www.turbomole.com>.
- 46 R. Ahlrichs, M. Bär, M. Häser, H. Horn and C. Kölmel, *Chem. Phys. Lett.*, 1989, **162**, 165–169.
- 47 C. Møller and M. S. Plesset, *Phys. Rev.*, 1934, **46**, 618–622.
- 48 F. Weigend, M. Häser, H. Patzelt and R. Ahlrichs, *Chem. Phys. Lett.*, 1998, **294**, 143–152.
- 49 F. Weigend and M. Häser, *Theor. Chem. Acc.*, 1997, **97**, 331–340.
- 50 C. Hattig, *J. Chem. Phys.*, 2003, **118**, 7751–7761.
- 51 O. Christiansen, H. Koch and P. Jørgensen, *Chem. Phys. Lett.*, 1995, **243**, 409–418.
- 52 J. T. H. Dunning, *J. Chem. Phys.*, 1989, **90**, 1007–1023.
- 53 A. E. Reed, R. B. Weinstock and F. Weinhold, *J. Chem. Phys.*, 1985, **83**, 735–746.
- 54 O. Dominguez, B. Rodriguez-Molina, M. Rodriguez, A. Ariza, N. Farfan and R. Santillan, *New J. Chem.*, 2011, **35**, 156–164.
- 55 G. Grivani, A. D. Khalaji, V. Tahmasebi, K. Gotoh and H. Ishida, *Polyhedron*, 2012, **31**, 265–271.
- 56 J. M. Fernández-G, F. del Rio-Portilla, B. Quiroz-García, R. A. Toscano and R. Salcedo, *J. Mol. Struct.*, 2001, **561**, 197–207.
- 57 A. Filarowski, T. Głowiaka and A. Koll, *J. Mol. Struct.*, 1999, **484**, 75–89.
- 58 H. Fukuda, K. Amimoto, H. Koyama and T. Kawato, *Org. Biomol. Chem.*, 2003, **1**, 1578–1583.
- 59 H. Tanak, *J. Phys. Chem. A*, 2011, **115**, 13865–13876.
- 60 A. L. Sobolewski and W. Domcke, *Chem. Phys. Lett.*, 2008, **457**, 404–407.
- 61 A. L. Sobolewski and W. Domcke, *ChemPhysChem*, 2007, **8**, 756–762.
- 62 S. Yamazaki, A. L. Sobolewski and W. Domcke, *Phys. Chem. Chem. Phys.*, 2009, **11**, 10165–10174.